Molecular and Solid-State Tests of Density Functional Approximations: LSD, GGAs, and Meta-GGAs

STEFAN KURTH,[1] JOHN P. PERDEW,[1] PETER BLAHA[2]

[1]*Department of Physics and Quantum Theory Group, Tulane University, New Orleans, Louisiana 70118*
[2]*Institute for Technical Electrochemistry, Technical University Vienna, A-1060 Vienna, Austria*

ABSTRACT: Results from numerical tests of nine approximate exchange–correlation energy functionals are reported for various systems—atoms, molecules, surfaces, and bulk solids. The functional forms can be divided into three categories: (1) the local spin density (LSD) approximation, (2) generalized gradient approximations (GGAs), and (3) meta-GGAs. In addition to the spin densities and their first gradients, the input to a meta-GGA includes other semilocal information such as Laplacians of the spin densities or orbital kinetic energy densities. We present a way to visualize meta-GGA nonlocality which generalizes that for GGA nonlocality, and which stresses the different meta-GGA descriptions of iso-orbital and orbital overlap regions of space. While some of the tested approximations were constructed semiempirically with many parameters fitted to chemical data, others were constructed to incorporate key properties of the exact exchange–correlation energy. The latter functionals perform well for both small and extended systems, with the best performance achieved by a meta-GGA which recovers the correct gradient expansion. While the semiempirical functionals can achieve high accuracy for atoms and molecules, they are typically less accurate for surfaces and solids. © 1999 John Wiley & Sons, Inc. Int J Quant Chem 75: 889–909, 1999

Key words: density functional; exchange–correlation; local spin density approximation; generalized gradient approximation; molecules; solids; surfaces

Introduction

Density functional theory [1–4] has become a widely used tool for calculating the electronic structure of systems of very different physical nature, such as atoms, molecules, surfaces, and solids. In this theory, the ground-state energy E of a system of interacting electrons is written as a functional of the densities n_σ of electrons of spin σ:

$$E = T_s[n_\uparrow, n_\downarrow] + \int d^3r\, v(\mathbf{r}) n(\mathbf{r})$$
$$+ \frac{1}{2} \int d^3r \int d^3r'\, \frac{n(\mathbf{r})n(\mathbf{r}')}{|\mathbf{r} - \mathbf{r}'|} + E_{xc}[n_\uparrow, n_\downarrow], \quad (1)$$

where $v(\mathbf{r})$ is the external potential of the nuclei, $n(\mathbf{r}) = n_\uparrow(\mathbf{r}) + n_\downarrow(\mathbf{r})$ is the total density of the electrons, $T_s[n_\uparrow, n_\downarrow]$ is the kinetic energy of a system of noninteracting electrons with spin densities $n_\uparrow$ and $n_\downarrow$, and $E_{xc}[n_\uparrow, n_\downarrow]$ is the exchange–correlation energy. The nucleus–nucleus repulsion not shown explicitly in Eq. (1) is also part of the total energy E. The spin densities can be calculated via

$$n_\sigma(\mathbf{r}) = \sum_i^{occ} |\varphi_{i\sigma}(\mathbf{r})|^2, \quad (2)$$

where the orbitals $\varphi_{i\sigma}$ are self-consistent solutions of the Kohn–Sham equation

$$\left(-\frac{\nabla^2}{2} + v(\mathbf{r}) + \int d^3r'\, \frac{n(\mathbf{r}')}{|\mathbf{r} - \mathbf{r}'|} + v_{xc}^\sigma(\mathbf{r}) \right) \varphi_{i\sigma}(\mathbf{r})$$
$$= \varepsilon_{i\sigma}\, \varphi_{i\sigma}(\mathbf{r}). \quad (3)$$

Here the exchange–correlation potential $v_{xc}^\sigma(\mathbf{r})$ is the functional derivative of the exchange–correlation energy:

$$v_{xc}^\sigma(\mathbf{r}) = \frac{\delta E_{xc}[n_\uparrow, n_\downarrow]}{\delta n_\sigma(\mathbf{r})}. \quad (4)$$

The kinetic energy T_s can be expressed exactly in terms of the Kohn–Sham orbitals $\varphi_{i\sigma}$, i.e.,

$$T_s[n_\uparrow, n_\downarrow] = \sum_{i\sigma}^{occ} \int d^3r\, \varphi_{i\sigma}^*(\mathbf{r}) \left(-\frac{\nabla^2}{2} \right) \varphi_{i\sigma}(\mathbf{r}). \quad (5)$$

Therefore, the only unknown piece of the total energy of Eq. (1) is the exchange–correlation energy functional $E_{xc}[n_\uparrow, n_\downarrow]$, which must be approximated in practical applications.

The early success of density functional theory can be attributed to the fact that the simplest approximation to E_{xc}, the local spin density (LSD) approximation [2, 5], has proved to be remarkably accurate. It has been the workhorse of solid-state electronic structure theory for many years. In LSD, the exchange–correlation energy is written as

$$E_{xc}^{LSD}[n_\uparrow, n_\downarrow] = \int d^3r\, n(\mathbf{r}) \epsilon_{xc}^{unif}\big(n_\uparrow(\mathbf{r}), n_\downarrow(\mathbf{r}) \big), \quad (6)$$

where $\epsilon_{xc}^{unif}(n_\uparrow, n_\downarrow)$ is the exchange–correlation energy per particle of a uniform electron gas with spin densities $n_\uparrow$ and $n_\downarrow$. This quantity is known very accurately from quantum Monte Carlo calculations [6].

Although LSD had been in widespread use in solid-state physics, it took the advent of generalized gradient approximations (GGAs) [7–13] with their improved accuracy to make density functional theory popular in quantum chemistry as well. GGAs express the exchange–correlation energy in terms of the spin densities and their local gradients, i.e.,

$$E_{xc}^{GGA}[n_\uparrow, n_\downarrow] = \int d^3r\, n(\mathbf{r}) \epsilon_{xc}^{GGA}$$
$$\times (n_\uparrow, n_\downarrow, \nabla n_\uparrow, \nabla n_\downarrow). \quad (7)$$

While ϵ_{xc}^{unif} in Eq. (6) is uniquely defined, there is no unique input function ϵ_{xc}^{GGA} to define GGA and many forms have been proposed.

More recently, yet another type of approximation to E_{xc} has shown promise. These approximations [14–27], which will be called meta-GGAs (MGGAs) [26], require additional semilocal information such as Laplacians of the spin densities or kinetic energy densities as input, i.e.,

$$E_{xc}^{MGGA}[n_\uparrow, n_\downarrow]$$
$$= \int d^3r\, n(\mathbf{r}) \epsilon_{xc}^{MGGA}$$
$$\times \big(n_\uparrow, n_\downarrow, \nabla n_\uparrow, \nabla n_\downarrow,$$
$$\times \nabla^2 n_\uparrow, \nabla^2 n_\downarrow, \tau_\uparrow, \tau_\downarrow \big), \quad (8)$$

where the kinetic energy density is defined by

$$\tau_\sigma(\mathbf{r}) = \frac{1}{2} \sum_i^{occ} |\nabla \varphi_{i\sigma}(\mathbf{r})|^2. \quad (9)$$

Equivalently

$$\tau_\sigma(\mathbf{r}) = \sum_i^{occ} \varepsilon_{i\sigma} |\varphi_{i\sigma}(\mathbf{r})|^2 - v_{eff}^\sigma(\mathbf{r}) n_\sigma(\mathbf{r}) + \tfrac{1}{4}\nabla^2 n_\sigma(\mathbf{r}),$$

(10)

where $v_{eff}^\sigma(\mathbf{r})$ is the spin-dependent effective or Kohn–Sham potential of Eq. (3). τ is, of course, an ingredient of the Colle–Salvetti correlation functional [28] (but see Refs. [29] and [30]), and of the Skyrme interaction in nuclear physics [31]. Early meta-GGAs [32, 33] preceded most GGAs. The current revival of interest in meta-GGAs may be due to Salahub and collaborators [20, 22]. A sound theoretical base for a meta-GGA is provided by the fourth-order gradient expansion of the exchange energy [34].

"Meta" is used here in the sense of "beyond," "occurring in succession to," and "more comprehensive: transcending." Note that $\tau_\sigma(\mathbf{r})$ is a functional of $n_\sigma(\mathbf{r})$, as are the potential $v_{eff}^\sigma(\mathbf{r})$ and orbital energies $\varepsilon_{i\sigma}$ in Eq. (10).

Here we also mention the so-called hybrid functionals [35–42], which mix a fraction of the exact exchange energy:

$$E_x = -\frac{1}{2} \sum_\sigma \sum_{i,j}^{occ} \int d^3r \int d^3r'$$

$$\times \frac{\varphi_{i\sigma}^*(\mathbf{r})\varphi_{j\sigma}^*(\mathbf{r}')\varphi_{i\sigma}(\mathbf{r}')\varphi_{j\sigma}(\mathbf{r})}{|\mathbf{r}-\mathbf{r}'|} \quad (11)$$

with some GGA for the remaining part of E_{xc}, e.g.,

$$E_{xc}^{hyb}[n_\uparrow, n_\downarrow] = a(E_x - E_x^{GGA}) + E_{xc}^{GGA}, \quad (12)$$

and have in recent years become popular mostly in quantum chemistry.

Here we pause to define the terms "locality," "semilocality," and "nonlocality," as used in this work. As in Eqs. (6)–(8) or (11), we write E_{xc} as an integral over $\mathbf{r}$ of a function of $\mathbf{r}$ which we shall call an energy density. A "local functional of the density" (e.g., LSD) is one in which the energy density at $\mathbf{r}$ is determined by the electron density at $\mathbf{r}$. A "semilocal functional of the density" (e.g., GGA) is one in which the energy density at $\mathbf{r}$ is determined by the electron density in an infinitesimal neighborhood of $\mathbf{r}$. A "nonlocal functional of the density" (e.g., exact exchange) is one in which the energy density at $\mathbf{r}$ is determined by the electron density at finite displacements away from $\mathbf{r}$. (The Kohn–Sham orbitals and their kinetic energy density are also nonlocal functionals of the den-

sity.) Much of the computational convenience of density functional theory arises from the semilocality of approximate functionals. However, this convenience is retained even by nonlocal functionals of the density, such as the meta-GGAs which employ τ, so long as the energy density at $\mathbf{r}$ is computed from the density *and the orbitals* in an infinitesimal neighborhood of $\mathbf{r}$. This "semilocal information" is readily found and used in any Kohn–Sham calculation, and such functionals are still "semilocal functionals of the density and the orbitals," even if they are not "semilocal functionals of the density." (Originally, GGAs were called "nonlocal approximations." Kohn [43] has described GGAs as "quasi-local"; "quasi" and "semi" are synonymous. So far as we know, the first use of "semilocal" in density functional theory was in Ref. [44], while the first use of "generalized gradient approximation" was in Ref. [9].)

In this study, we will report numerical results from LSD, four GGAs, and four meta-GGAs, for a variety of systems of very different physical nature, such as atoms, molecules, surfaces, and solids. However, we will not report results for any hybrid functionals. Becke's recent functionals [37, 45] which are inextricably hybridized, have not been included in our study. Many GGAs and meta-GGAs have also been omitted for reason of economy. Inclusion does not signify our approval, and omission does not signify our disapproval.

Some of the functionals we tested have been designed to give accurate results for atoms or atomization energies of molecules, sometimes with the use of many fit parameters. These functionals have rarely or never been tested in solid-state calculations before. Other functionals we used have been constructed less or nonempirically to satisfy key properties of the exact exchange–correlation functional. Key properties are those which, if satisfied globally for all possible electron densities, help to constrain the approximation to realistic energies for realistic densities. In particular, everything right about LSD should be preserved beyond LSD.

In the next section we will briefly describe each of the approximations studied in this work. In the third section we will present the numerical results. In the fourth section we will give an overall discussion of the results and close with some general thoughts on the construction of approximate functionals.

In some of our numerical tests, we apply meta-GGA energy functionals to LSD or GGA orbitals

and densities. For total energies or energy differences, such ''post-LSD'' or ''post-GGA'' calculations are protected by the Hohenberg–Kohn variational principle [1], as confirmed by many practical tests in quantum chemistry [46] and solid-state physics. Because the orbital kinetic energy density τ is not known as an explicit functional of the electron density, the functional derivative of the meta-GGA of Eq. (8) is not easily evaluated. Fully self-consistent calculations for the meta-GGAs which employ τ will require construction of the exchange–correlation potential from the orbitals by the optimized effective potential (OEP) method [47–49] or use of the Neumann–Nobes–Handy method [50], and have not been attempted here.

Brief Description of the Approximations

LOCAL SPIN DENSITY APPROXIMATION

The local spin density approximation of Eq. (6) is based on the uniform electron gas. LSD approximates the exchange–correlation energy density of a real, spatially inhomogeneous system at each point $\mathbf{r}$ in space by that of a uniform electron gas with spin densities equal to the local $n_\uparrow(\mathbf{r})$ and $n_\downarrow(\mathbf{r})$. The exchange–correlation energy per particle of a uniform electron gas, $\epsilon_{xc}^{unif}(n_\uparrow, n_\downarrow)$, is known from quantum Monte Carlo calculations [6]. These results have been parametrized [51–53] for convenient use in practical calculations. We use the parametrization of Perdew and Wang [53], but the others are not very different.

As already mentioned above, the simple LSD has been remarkably successful in practical applications. This success outside its formal domain of validity (very slowly varying densities) can be attributed to the fact that LSD satisfies many formal properties of the exact exchange–correlation energy functional. Probably the most important of these properties are the sum rules for the exchange and correlation holes and the on-top hole densities [54]. The Lieb–Oxford bound [55] for E_{xc} is satisfied by LSD, which also provides a surprisingly good account of the linear response of a spin-unpolarized uniform electron gas [56].

GENERALIZED GRADIENT APPROXIMATIONS

We have tested four GGAs. All are of the form of Eq. (7), with different choices for the function ϵ_{xc}^{GGA}.

Perdew, Burke, and Ernzerhof

The nonempirical GGA of Perdew, Burke, and Ernzerhof (PBE) [13] is constructed to retain the correct features of LSD while adding others. It retains the correct uniform-gas limit, the correct spin- and uniform-density scaling of E_x, the correct upper bounds $E_x < 0$ and $E_c \leq 0$ and the correct Lieb–Oxford lower bound [57], and the LSD linear response. In addition, the PBE correlation energy functional reduces to the correct second-order gradient expansion [58–60] in the slowly varying limit. Furthermore, under uniform scaling of the density [$n(\mathbf{r}) \to \lambda^3 n(\lambda \mathbf{r})$] the PBE correlation energy correctly [61] scales to a constant in the limit $\lambda \to \infty$. Although the sum rules for the exchange and correlation holes do not explicitly enter into its derivation, the PBE functional closely resembles that of Perdew and Wang 1991 (PW91) [12, 44]. The latter functional is an analytic fit to a numerical GGA [62] obtained by real-space cutoff of the spurious long-range parts of the second-order gradient expansion of the exchange–correlation hole, with the cutoffs chosen to satisfy the sum rules on the exact hole.

Less happily, the PBE exchange functional does not reduce to the correct second-order gradient expansion in the slowly varying limit. The GGA form is too restricted to obtain this limit correctly and to reproduce the realistic LSD uniform-gas linear response simultaneously. The LSD linear response was retained in PBE because it appeared to be energetically more important than the correct slowly varying limit for exchange and because this is the ''choice'' made by LSD.

Revised PBE (RPBE)

Recently, Hammer, Hansen, and Norskov [63] suggested a slightly modified version of the PBE GGA. This revised PBE (RPBE) functional uses the same correlation functional as PBE, but the enhancement factor for exchange is chosen differently (see Eq. (15) of Ref. [63]). RPBE preserves many of the correct features of the original PBE functional (slowly varying limit of the correlation energy functional, Lieb–Oxford bound, LSD linear response), but for intermediate values $1 \lesssim s \lesssim 3$ of the reduced density gradient

$$s = \frac{|\nabla n|}{2(3\pi^2)^{1/3} n^{4/3}} \qquad (13)$$

it does not follow the PW91 GGA (which results from the real-space cutoff) as closely as PBE does. In fact, RPBE and the earlier revPBE of Refs. [64, 65] more closely resemble Becke's exchange functional [10] in the range $1 \lesssim s \lesssim 3$. Note that values of s larger than 3 are not energetically important in real systems [66].

Becke, Lee, Yang, and Parr (BLYP)

The BLYP functional combines Becke's exchange functional [10] with the correlation functional of Lee, Yang, and Parr (LYP) [11]. It has been and still is very popular in quantum chemistry. Becke's exchange functional correctly reproduces the LSD limit for uniform systems, but (like PBE) it does not give the correct gradient coefficient in the slowly varying limit. The Becke gradient coefficient is determined semiempirically by fitting to exact exchange energies of six noble-gas atoms.

The correlation functional of Lee, Yang, and Parr is a simplification of the Colle–Salvetti correlation functional [67]. While the latter functional explicitly depends on the single-particle orbitals, the functional of Lee, Yang, and Parr is written in terms of the spin densities and their first gradients only. It contains four semiempirical parameters, all from the underlying Colle–Salvetti functional and obtained by a fitting procedure involving the helium atom. Although this functional (in combination with Becke's exchange) has been applied very successfully in quantum chemistry, from a fundamental point of view it has some serious disadvantages: (1) LYP does not reduce to the correct uniform limit, and (2) the LYP correlation energy vanishes identically for any completely spin-polarized system. While this vanishing correlation energy is correct for any one-electron system, it is otherwise incorrect.

Hamprecht, Cohen, Tozer, and Handy

Recently, Hamprecht, Cohen, Tozer, and Handy (HCTH) [68] proposed a highly parametrized GGA for the exchange–correlation functional. It is based on a functional form proposed by Becke [45], but without exact exchange mixing. The HCTH functional contains 18 parameters which were obtained by fitting to a large set of experimental chemical data, e.g., total atomic energies, molecular atomization energies, and nuclear gradients for molecules at equilibrium geometries.

Apparently this functional has been designed to push the GGA form to its limits. However, many of the exact limiting cases of the exact exchange–correlation functional have not been taken into account in its construction. The uniform limit is not reproduced, nor are the second-order gradient coefficients for exchange or correlation. In addition, the experimental data set, from which the fit parameters are obtained, is dominated by chemical properties of rather small systems (atoms and molecules).

Picturing GGA Nonlocality

The effect of nonlocality can be visualized for the GGAs by plotting the s dependence of the enhancement factor F_{xc} over local exchange, defined through

$$E_{xc}^{GGA}[n_\uparrow, n_\downarrow] = \int d^3 r\, n(\mathbf{r}) \epsilon_x^{unif}(n) F_{xc}^{GGA}(r_s, \zeta, s).$$

$$(14)$$

Here,

$$\epsilon_x^{unif}(n) = -\frac{3}{4\pi}(3\pi^2 n)^{1/3} \qquad (15)$$

is the exchange energy per particle of the unpolarized uniform electron gas,

$$r_s = \left(\frac{3}{4\pi n}\right)^{1/3} \qquad (16)$$

is the density parameter, $\zeta = (n_\uparrow - n_\downarrow)/(n_\uparrow + n_\downarrow)$ is the relative spin polarization, and s is the reduced density gradient defined in Eq. (13). Valence electrons typically have $2 \lesssim r_s \lesssim 10$; the high- and low-density limits are $r_s \to 0$ and $r_s \to \infty$, respectively. Plots of the enhancement factors for the GGAs tested in this study have been published elsewhere: for PBE in Fig. 1 of Ref. [13], for RPBE exchange in Fig. 3(a) of Ref. [63], for BLYP in Fig. 6 of Ref. [69], and for HCTH in Fig. 1 of Ref. [68].

Since LSD corresponds to the choice $F_{xc}^{LSD}(r_s, \zeta, s) = F_{xc}^{GGA}(r_s, \zeta, 0)$ for a properly constructed GGA, the s dependence of F_{xc}^{GGA} displays the nonlocality of the GGA functional.

META-GGAS

Whereas GGAs use n_σ and $|\nabla n_\sigma|$ as input, meta-GGAs add τ_σ or $\nabla^2 n_\sigma$. For slowly varying

densities, τ_σ and $\nabla^2 n_\sigma$ bring the same additional information, since τ_σ of Eq. (9) has the gradient expansion [70]

$$\tau_\sigma = \frac{3}{10}(6\pi^2)^{2/3} n_\sigma^{5/3} + \frac{1}{72}\frac{|\nabla n_\sigma|^2}{n_\sigma} + \frac{1}{6}\nabla^2 n_\sigma + O(\nabla^4). \quad (17)$$

For any density, Becke has argued that τ_σ plays an important role in the exchange [71] and correlation [72] energies. In 1985, Jones and Gunnarson [73] stated that ''modifications of the local density approximation which do not consider the nature of the orbitals involved are unlikely to be satisfactory in all systems.'' Meta-GGAs that use the kinetic energy density τ of Eq. (9) are explicitly orbital-dependent in a way that GGAs are not. However, because the Kohn–Sham orbitals are functionals of the density, these meta-GGAs are still density functionals. Four meta-GGAs have been tested in this work.

Perdew, Kurth, Zupan, and Blaha

The meta-GGA proposed by Perdew, Kurth, Zupan, and Blaha (PKZB) [26] expresses the exchange–correlation functional not only in terms of the spin densities and their gradients but also in terms of the kinetic energy densities for each spin. It correctly reproduces the uniform limit, and its exchange part reproduces the fourth-order gradient expansion [18, 34] for slowly varying densities. This meta-GGA recovers the exact linear response function $\gamma_x(k)$ (as defined in Ref. [74]) up to fourth order in $k/(2k_F)$, where k_F is the Fermi wavevector. Due to the flexibility gained by the introduction of the kinetic energy densities as new variables, the combined exchange–correlation linear response function $\gamma_{xc}(k)$ of this meta-GGA is in good agreement with nearly exact results for $0 \leq k/2k_F \leq 1.5$. Thus the PKZB meta-GGA exchange retains all the correct features of the PBE GGA exchange, and adds a correct gradient expansion.

The PKZB correlation functional is based on the PBE correlation functional and retains its correct features. In addition, PKZB correlation is free of self-interaction error, i.e., the correlation energy correctly vanishes for any one-electron density [52]. The self-correlation error of LSD and GGA seems to be the principal source of error of those func-

tionals in the strongly interacting limit [75]. (Note that the self-exchange error cannot be eliminated within the meta-GGA form.)

The PKZB functional contains two fitted parameters. One of these parameters is fixed by the theoretical condition that the self-interaction correction should have no effect for extended systems like the jellium surface. The second parameter (the only unknown fourth-order gradient coefficient in the gradient expansion for exchange) is then obtained by minimizing the mean absolute error in the atomization energies of 20 small molecules. However, the resulting value for this parameter (or at least its order of magnitude) is also supported by studies of the surface exchange energies for slowly varying densities [76]. We regard PKZB as a controlled extrapolation away from the slowly varying limit, like LSD and PBE GGA but with greater sophistication.

Krieger, Chen, Iafrate, and Savin

Krieger, Chen, Iafrate, and Savin (KCIS) [25] have constructed a meta-GGA correlation functional based on the idea of a uniform electron gas with a gap in the excitation spectrum. This functional also preserves many of the known properties of the exact correlation energy: It reduces to the correct uniform limit, it is free of self-interaction, and it scales to a constant under uniform density scaling to the high-density limit. The KCIS work reawakened one of us (J.P.P.) to the importance of the self-interaction correction. However, it appears that for slowly varying densities the self-interaction-corrected KCIS functional only reproduces the correct gradient coefficient in the high-density limit. Appendix A displays the KCIS functional, which because of length limits was not fully displayed in Ref. [25].

Since KCIS do not suggest any form for the exchange energy functional, we have tested their functional in combination with the exchange functional of PKZB. This was done, however, without reoptimizing the parameter in the PKZB exchange.

Van Voorhis and Scuseria

The meta-GGA of Van Voorhis and Scuseria (VS98) [23] uses as input the same variables as the PKZB or KCIS functionals. In fact, the remarkable accuracy of the VS98 functional for molecular atomization energies was one of the inspirations for

the PKZB work. The functional form of VS98 exchange is based on a density-matrix expansion [77, 78], which is then modified through the introduction of fit parameters. The correlation functional is self-interaction free, with its functional form otherwise taken to be similar to that for exchange.

The VS98 functional satisfies some exact conditions (e.g., nonuniform density scaling of E_x) which even the PKZB functional does not. However, neither the exchange nor the correlation piece of the VS98 functional is exact in the uniform or slowly varying limit. This functional contains many (21) parameters which are obtained by fitting to chemical data. Just as in the case of the highly parametrized HCTH functional, no information about extended systems has been included in the fit.

Filatov and Thiel

The meta-GGA proposed by Filatov and Thiel (FT98) [24] does not use the kinetic energy densities but rather uses reduced Laplacians of the densities,

$$q_\sigma = \frac{\nabla^2 n_\sigma}{4(3\pi^2)^{2/3} n_\sigma^{5/3}}, \qquad (18)$$

as semilocal input information in addition to the spin densities and the first reduced gradients. The FT98 exchange functional correctly reproduces LDA exchange in the uniform limit and the correct second-order exchange coefficient in the slowly varying limit. It even gives the correct fourth-order coefficient for the q^2 term, but not the other two fourth-order coefficients. The exchange functional contains four parameters obtained by fitting to 10 atomic exchange energies.

The FT98 correlation functional originates [79] from a model of the correlation hole of the uniform electron gas. The effect of the inhomogeneity is then introduced [24] via an empirical ansatz for the effective correlation length. This ansatz contains four more parameters which were obtained by fitting to atomic correlation energies.

The construction of the FT98 functional requires the parametrization of the uniform gas correlation energies given by the authors in Ref. [79] and not that of Perdew and Wang [53]. However, both parametrizations are very close to each other, as can be seen from Table II of Ref. [79].

Picturing Meta-GGA Nonlocality: Metaphysics

Due to the larger number of variables, meta-GGAs are more difficult to visualize than GGAs. However, meta-GGAs using the kinetic energy density of Eq. (9) are able to distinguish between ''iso-orbital'' and ''orbital overlap'' regions of space and can be brought into GGA form for those regions. Iso-orbital and orbital overlap regions can be mapped with the help of the ''electron localization function'' of Ref. [80]. Here we define an iso-orbital region as a region of space where the spin densities are dominated by one orbital or by several orbitals of the same shape. In this case, the kinetic energy density for spin σ is given to a good approximation by the Weizsäcker form, i.e.,

$$\tau_\sigma(\mathbf{r}) \approx \tau_\sigma^W(\mathbf{r}) = \frac{1}{8} \frac{|\nabla n_\sigma(\mathbf{r})|^2}{n_\sigma(\mathbf{r})}. \qquad (19)$$

Iso-orbital regions can be found, e.g., in density tails of atoms, in the bond regions of singly bonded molecules, or in lone pairs. We have plotted the enhancement factors of the PKZB, KCIS, and VS98 functionals in iso-orbital regions for spin-unpolarized systems and fully spin-polarized systems in Figures 1 and 2, respectively. The PKZB, KCIS, and VS98 meta-GGAs were all constructed to give a vanishing correlation energy for any one-electron system. For these systems all space is an iso-orbital region, leaving an enhancement factor which is independent of the density parameter r_s. Since we use the same exchange functional for the PKZB and KCIS meta-GGAs, only two curves must be shown in Figure 2.

While the kinetic energy density can be accurately represented by the Weizsäcker form in iso-orbital regions, there is no precise way to represent τ_σ in terms of n_σ and ∇n_σ alone for orbital overlap regions of space, e.g., intershell regions in atoms, regions of multiple-bond congestion in molecules, or interstitial and surface regions in metals. However, to have some visualization for these regions as well, we have brought the meta-GGAs into GGA form by plotting the enhancement factors for

$$\tau_\sigma = \frac{3}{10}(6\pi^2)^{2/3} n_\sigma^{5/3} + \frac{1}{8} \frac{|\nabla n_\sigma|^2}{n_\sigma}. \qquad (20)$$

This choice was made because it gives the correct limit for uniform densities and simultaneously sat-
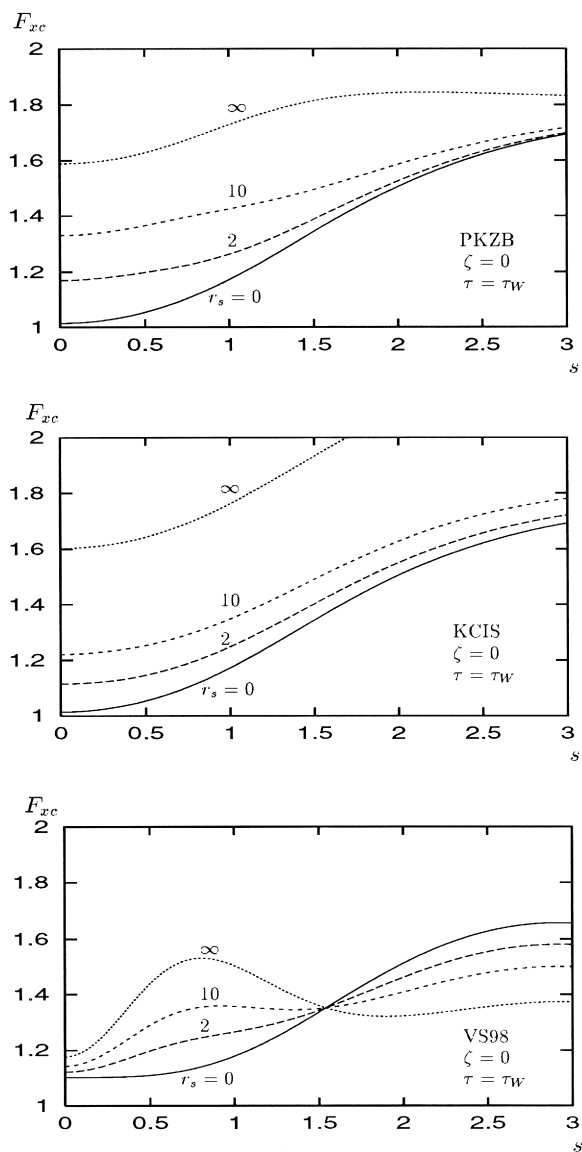
FIGURE 1. Enhancement factors F_{xc} of Eq. (14) for several meta-GGAs at zero spin polarization $\zeta = 0$, in iso-orbital regions where the kinetic energy density τ is given by the Weizsäcker form of Eq. (19). s is the reduced density gradient of Eq. (13), and r_s is the density parameter of Eq. (16). The $r_s = 0$ curve is the exchange-only enhancement factor.

isfies the exact condition

$$\tau_\sigma \geq \tau_\sigma^W. \tag{21}$$

Equation (21) is proved in Appendix B. The corresponding enhancement factors for the meta-GGAs with τ_σ given by Eq. (20) are shown for zero and full-spin polarization in Figures 3 and 4, respectively.
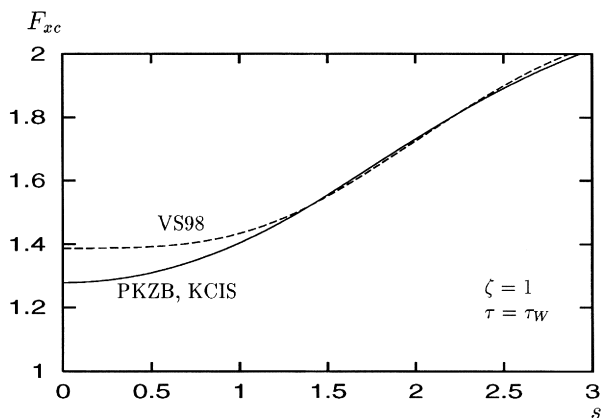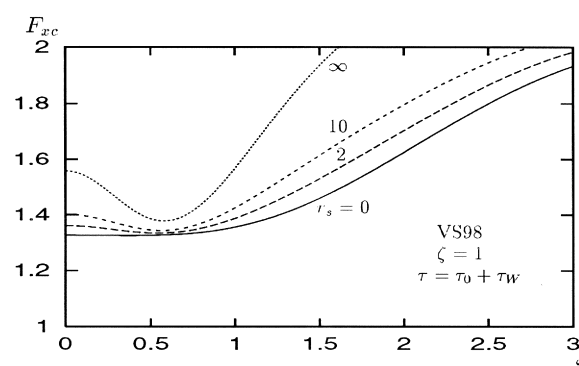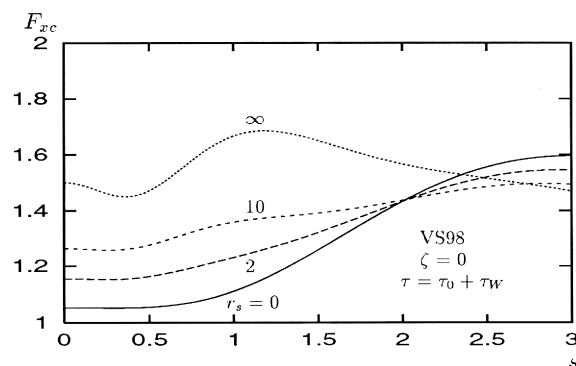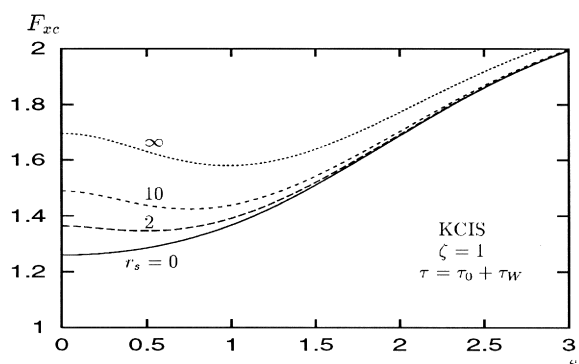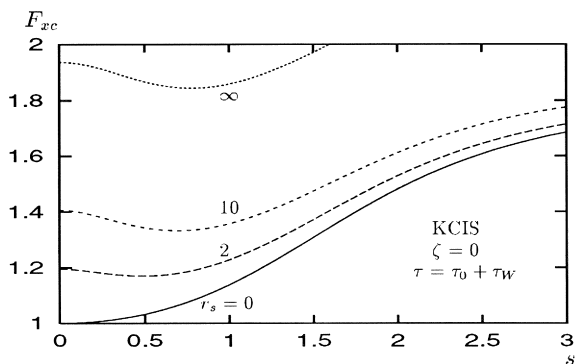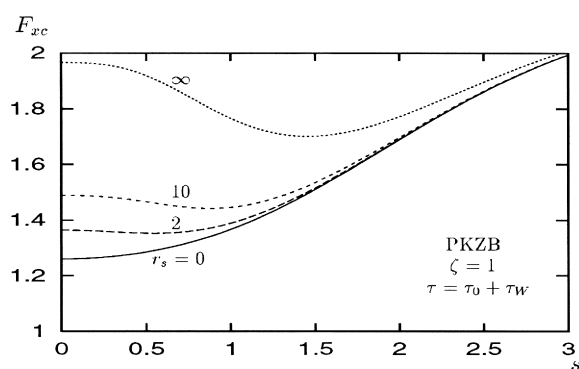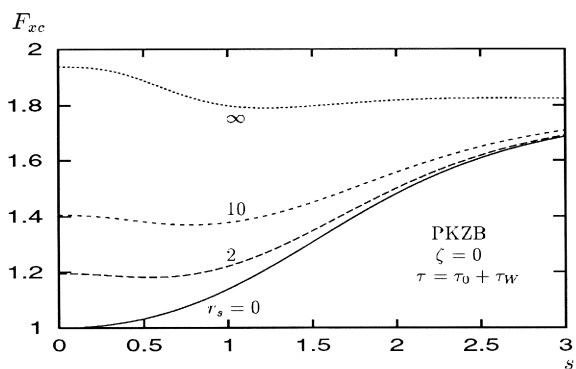

FIGURE 2. Same as Figure 1, but for full spin polarization $\zeta = 1$. Since in this case the correlation energy vanishes identically for the PKZB, KCIS, and VS98 functionals, the enhancement factors become independent of r_s.

Figures 1–4 show that, as for the PBE GGA [74], the exchange energy of the PKZB meta-GGA turns on, and its correlation energy turns off relative to exchange, as the inhomogeneity parameter s or the spin polarization ζ increases, or as the density parameter r_s decreases. Comparison of Figure 3 with Figure 1 is instructive. The PKZB, KCIS, and VS98 meta-GGAs all agree that exchange (the $r_s = 0$ curve) strengthens and correlation weakens as we pass from an orbital overlap region (Fig. 3) to an iso-orbital region (Fig. 1). This is reasonable: When an electron is in a single electron-pair bond, its exchange hole is localized to that bond, and the parallel-spin component of its correlation energy is suppressed. There is some qualitative agreement between the PKZB and KCIS curves, both of which are constructed from theoretical considerations, but these two functionals are rather different from the semiempirical VS98. The VS98 enhancement factors for $r_s > 0$ even dip below that for $r_s = 0$ at large s, showing that the VS98 correlation energy density can be positive.

The PKZB enhancement factors in Figures 3 and 4 display a negative second derivative with respect to s at $s = 0$. The small-s behavior of the PKZB panels of Figures 3 and 4 is that predicted by the first-principles second-order gradient expansion. This behavior is most evident at $r_s = \infty$, but should be visible at any r_s if plotted on a sufficiently fine scale. (Note that, in a gradient expansion of E_{xc}^{PKZB}, τ does not contribute to the ∇^0 and ∇^2 terms.)

FIGURE 3. Enhancement factors of Eq. (14) for several meta-GGAs at zero spin polarization in orbital overlap regions. The $r_s = 0$ curve is the exchange-only enhancement factor.

FIGURE 4. Same as Figure 3, but for full spin polarization.

To a GGA, ''a gradient is a gradient is a gradient'' in the words of Kohn (see also Ref. [81]), but, to a meta-GGA, a density and its gradient in an iso-orbital region are not the same as in an orbital overlap region.

Although not designed to do so, meta-GGAs might help to solve a problem pointed out in Ref. [82]: An insulating crystal can support a weak macroscopic electric field over a large interior volume. Within this volume, there is a periodic elec-

tron density which does not uniquely determine the exchange hole around an electron, since the same periodic density can be constructed from Kohn–Sham potentials with or without a macroscopic Kohn–Sham electric field. The orbitals, however, must sense the macroscopic field; otherwise the exchange hole would not sense it. Although τ of Eq. (9) is found semilocally in a Kohn–Sham calculation (via differentiation of the orbitals), it is a fully nonlocal functional of the density, as are the orbitals.

Numerical Results

UNIFORM ELECTRON GAS

The uniform electron gas plays a special role for semilocal functionals (GGAs, meta-GGAs): It is the only system for which these functionals can be exact. (More generally, GGAs and meta-GGAs can be essentially exact for any slowly varying density.) As pointed out in the previous section, the BLYP, HCTH, and VS98 functionals do not reduce to the correct uniform limit for constant spin densities. In Figure 5 we show the exchange–correlation energy per particle obtained with these functionals as a function of the density parameter r_s of Eq. (16), and compare them to the essentially exact LSD result obtained from the Perdew-Wang parametrization [53]. The results obtained with the parametrization of Filatov and Thiel [79] are indistinguishable from the Perdew–Wang results on the scale of Figure 5.

The middle panel of Figure 5 shows the errors for the unpolarized case ($\zeta = 0$), while the lower panel shows the corresponding errors for the fully spin-polarized case ($\zeta = 1$). The BLYP functional gives the largest deviations from the exact results. This is particularly true for the fully spin-polarized case, where the BLYP correlation energy vanishes. Deviations from the exact results are not negligible. For example, at $r_s = 2$ one obtains the following relative errors in ϵ_{xc} for the unpolarized case: BLYP: 6.5%, HCTH: 0.7%, VS98: 3.4%, and for the fully polarized case: BLYP: 7.7%, HCTH: 2.7%, VS98: 0.2%. Interestingly, the HCTH and VS98 fitting to chemical data does provide some information about the physically different uniform electron gas.

ATOMS

We have performed self-consistent calculations for several spherically symmetric atoms, using a numerical code for the solution of the Kohn–Sham equation. In Tables I and II we show atomic exchange and correlation energies obtained from the different approximations. The functionals were evaluated with orbitals and densities obtained self-consistently from the exact-exchange-only optimized effective potential (OEP) method [47–49], which could be (but was not) modified to find self-consistent meta-GGA orbitals.
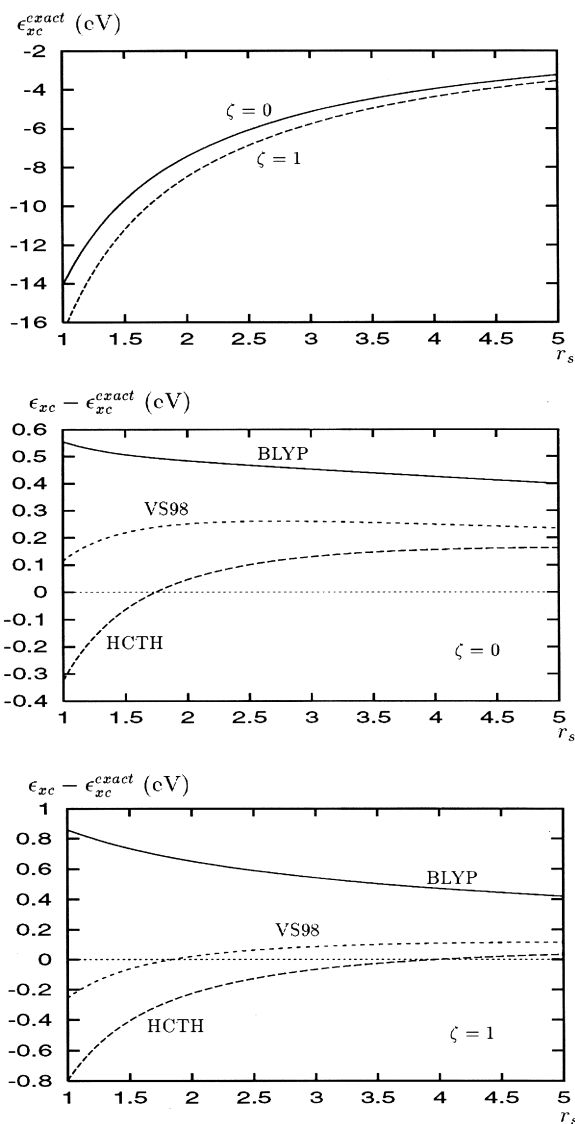
FIGURE 5. Exchange–correlation energy per particle of the unpolarized ($\zeta = 0$) and fully polarized ($\zeta = 1$) uniform electron gas. The upper panel shows the essentially exact results from the parametrization of Perdew and Wang [53] of the quantum Monte Carlo results [6]. The middle and lower panels show the errors for the BLYP, HCTH, and VS98 functionals for the unpolarized and fully polarized case, respectively.

The magnitudes of atomic exchange energies are underestimated by 5–15% in LSD. Not surprisingly, all the GGAs and meta-GGAs reduce this error significantly. Among the GGAs, RPBE and BLYP give the smallest errors (consistently less than 1%), while PBE errors tend to be small (less than 1%) for the heavier atoms and typically between 1 and 2% for the lighter atoms. HCTH

TABLE I _____
Exchange energies ($-E_x$ in hartree) for some spherically symmetric atoms.[a]

	E_x^{exact}	E_x^{LSD}	E_x^{PBE}	E_x^{RPBE}	E_x^{BLYP}	E_x^{HCTH}	E_x^{PKZB}	E_x^{VS98}	E_x^{FT98}
H	0.3125	0.2680	0.3059	0.3112	0.3098	0.3055	0.3081	0.3148	0.3120
He	1.0258	0.8840	1.0136	1.0313	1.0255	1.0063	1.0202	1.0399	1.0302
Li	1.7807	1.5379	1.7572	1.7876	1.7753	1.7454	1.7682	1.7893	1.7852
Be	2.6658	2.3124	2.6358	2.6801	2.6578	2.6114	2.6482	2.6579	2.6707
N	6.6044	5.9008	6.5521	6.6252	6.5961	6.5145	6.5255	6.5968	6.6045
Ne	12.1050	11.0335	12.0667	12.1593	12.1378	12.0114	11.9514	12.1404	12.1260
Na	14.0131	12.7859	13.9506	14.0528	14.0304	13.9009	13.8115	14.0374	14.0177
Mg	15.9884	14.6117	15.9147	16.0260	16.0005	15.8596	15.7448	15.9967	15.9862
P	22.6341	20.7931	22.5028	22.6369	22.6221	22.5016	22.2475	22.6365	22.6089
Ar	30.1747	27.8632	29.9961	30.1494	30.1535	30.0751	29.6437	30.1918	30.1429
Kr	93.8330	88.6245	93.4257	93.6645	93.8721	95.1802	92.2949	94.8248	93.8407
Xe	179.0635	170.5660	178.2450	178.5649	179.0427	183.2130	176.2574	181.6907	179.0636
mare (in %)		9.8	0.8	0.3	0.2	1.4	1.3	0.5	0.1

[a]All functionals were evaluated with self-consistent exchange-only OEP orbitals and densities [47]. Exact values, E_x^{exact}, were obtained by evaluating Eq. (11) with these orbitals. The "mare" is the mean absolute value of the relative error.

errors are typically in the 1–2% range. For the meta-GGAs, we have typical errors of 1–2% for PKZB and less than 1% for VS98 and FT98. That the FT98 functional gives a very accurate atomic exchange energy is not surprising, since many of the atoms of Table I were used to obtain the fit parameters of this functional.

For the heavier atoms, the PKZB exchange energy is less accurate than that of PBE, because the smaller second-order gradient term of PKZB cannot cancel as much of the LSD self-interaction error in the inert core. In an atom, a region of small first reduced density gradient s [Eq. (13)] is *not* a region of slowly varying density, because higher-order reduced gradients are large there.

Typical relative errors for atomic correlation energies are much larger than for atomic exchange energies. LSD overestimates correlation energies by as much as 300%. These errors are reduced to 10% or less by PBE and less than 5% for BLYP, except for Li where BLYP is off by 17%. HCTH overestimates atomic correlation energies by up to 80% for He. This error is somewhat smaller for heavier atoms, but still amounts to 30% for Ar. Among the meta-GGAs, KCIS shows the best performance, with errors consistently lower than 10%.

TABLE II _____
Correlation energies ($-E_c$ in hartree) for some spherically symmetric atoms.[a]

	E_c^{exact}	E_c^{LSD}	E_c^{PBE}	E_c^{BLYP}	E_c^{HCTH}	E_c^{PKZB}	E_c^{KCIS}	E_c^{VS98}	E_c^{FT98}
H	0.0000	0.0222	0.0060	0.0000	0.0132	0.0000	0.0000	0.0000	0.0000
He	0.0420	0.1125	0.0420	0.0438	0.0753	0.0473	0.0408	0.0399	0.0464
Li	0.0455	0.1508	0.0514	0.0534	0.0961	0.0544	0.0498	0.0626	0.0555
Be	0.0950	0.2240	0.0856	0.0945	0.1505	0.0936	0.0861	0.1251	0.0916
N	0.1858	0.4268	0.1799	0.1919	0.2772	0.1841	0.1805	0.2342	0.1912
Ne	0.3929	0.7428	0.3513	0.3835	0.5046	0.3635	0.3667	0.4344	0.3661
Na	0.3988	0.8010	0.3715	0.4083	0.5370	0.3821	0.3905	0.4671	0.3909
Mg	0.4424	0.8874	0.4110	0.4594	0.6080	0.4252	0.4364	0.5384	0.4411
P	0.5446	1.1127	0.5265	0.5664	0.7457	0.5377	0.5551	0.6897	0.5513
Ar	0.7314	1.4242	0.7067	0.7508	0.9533	0.7229	0.7457	0.9117	0.7277
Kr		3.2693	1.7672	1.7486	2.0788	1.7849	1.8875	1.9554	1.8037
Xe		5.1773	2.9184	2.7440	3.1789	2.9364	3.1269	3.0873	2.9468
mare (in %)		128.3	6.4	4.5	51.8	5.8	4.3	22.3	5.5

[a]All functionals were evaluated with self-consistent exchange-only OEP orbitals and densities [47]. Exact correlation energies are taken from Ref. [25]. The "mare" excludes H, Kr, and Xe.

PKZB and FT98 typically also give errors of less than 10%, except for the He and Li atoms. Again, the accuracy of the FT98 correlation functional for atomic systems is not surprising, since atomic correlation energies were used to obtain the fit parameters. VS98 correlation energies are less accurate, with typical errors ranging from 15 to as much as 30%.

MOLECULES

Molecular atomization energies are probably the quantities of greatest interest to quantum chemists. In Tables III and IV, we report atomization energies for 20 small molecules. To construct these tables, we used experimental bond lengths [13] and orbitals constructed from the PBE GGA exchange–correlation potential.

Exchange-only atomization energies are reported in Table III. The approximate values were found by zeroing out the correlation energy functionals, and the exact values were obtained using

Eq. (11). As expected from the analysis of Ref. [83], all the density functionals show a serious tendency to overbind at the exchange-only level, especially for the multiply bonded molecules like N_2 and O_2. LSD is by far the worst performer, and the PKZB meta-GGA is the best (although its mean absolute error of 24 kcal/mol is still unacceptable).

Much more satisfactory results are found in Table IV, which includes correlation. It is a well-known fact that LSD-xc overbinds molecules, with a large mean absolute error of 32 kcal/mol for our set of molecules. (In previous LSD calculations for molecules [26], we inadvertently used the parametrization of Vosko, Wilk, and Nusair [51] instead of the one of Perdew and Wang [53], but this has little effect on the results.) GGAs and meta-GGAs greatly reduce this overbinding. The PBE functional performs well for the singly bonded molecules like CH_4 or NH_3, but still overbinds multiply bonded molecules such as N_2 or O_2. RPBE typically further reduces PBE atomization energies, which is sometimes good (as for, e.g., N_2

TABLE III

Exchange-only atomization energies (in kcal / mol) of 20 small molecules.[a]

Molecule	ΔE^{exact}	ΔE^{LSD}	ΔE^{PBE}	ΔE^{RPBE}	ΔE^{BLYP}	ΔE^{HCTH}	ΔE^{PKZB}	ΔE^{VS98}	ΔE^{FT98}
H_2	84.0	81.5	84.8	85.8	85.4	88.3	85.8	87.2	88.0
LiH	33.9	33.6	36.9	36.8	36.2	32.9	34.6	34.6	33.4
CH_4	327.2	369.9	336.0	326.9	331.2	350.7	319.0	333.8	332.1
NH_3	199.5	255.0	227.4	218.9	222.6	230.2	209.5	209.9	220.5
OH	67.3	96.2	84.5	80.9	82.7	85.3	76.9	79.3	80.9
H_2O	154.6	212.9	183.9	176.4	180.5	192.9	169.7	184.5	177.4
HF	96.1	136.1	117.1	112.6	115.4	125.4	109.3	125.0	113.5
Li_2	3.5	6.5	6.4	6.7	3.9	2.4	5.2	−2.4	1.7
LiF	86.8	129.7	116.5	110.8	113.6	110.9	103.5	115.5	107.5
Be_2	−11.0	9.4	3.1	1.2	1.6	1.9	−1.3	−2.1	0.0
C_2H_2	290.6	382.7	333.0	318.5	325.5	342.5	307.4	325.4	319.7
C_2H_4	423.9	517.7	456.5	439.6	447.4	474.0	426.8	445.8	446.9
HCN	194.5	294.0	256.1	243.5	249.1	252.7	232.8	232.5	243.3
CO	169.2	261.9	224.0	213.1	218.7	227.6	207.0	218.4	212.9
N_2	110.2	211.4	184.1	173.6	177.6	169.8	164.1	145.8	173.2
NO	45.6	156.9	122.8	112.5	117.0	118.7	105.1	98.3	113.7
O_2	24.9	147.5	104.4	94.1	99.3	113.9	89.1	100.0	97.1
F_2	−43.3	64.0	32.5	24.7	28.8	34.1	21.7	25.0	31.3
P_2	31.8	98.4	73.1	66.1	70.1	69.4	66.2	50.6	72.0
Cl_2	15.5	68.2	39.8	33.7	37.0	48.6	34.0	36.0	38.2
mae		61.7	35.9	28.6	31.9	38.6	23.9	27.5	30.2
mare (in %)	—	109.9	69.1	58.9	60.0	71.0	51.6	60.3	60.8

[a]All functionals were evaluated on PBE-xc orbitals and densities at experimental geometries, but the correlation energy contributions were zeroed out. The calculations were performed with a modified version of the CADPAC program [111]. The Gaussian basis sets are of triple-zeta quality, with p and d polarization functions for hydrogen, and d and f polarization functions for first- and second-row atoms. The "mae" is the mean absolute error over all 20 molecules. (1 hartree = 627.5 kcal / mol). The "mare" excludes Be_2.

TABLE IV _____
Atomization energies (in kcal / mol) of 20 small molecules, including correlation as well as exchange.[a]

Molecule	ΔE^{expt}	ΔE^{LSD}	ΔE^{PBE}	ΔE^{RPBE}	ΔE^{BLYP}	ΔE^{HCTH}	ΔE^{PKZB}	ΔE^{KCIS}	ΔE^{VS98}	ΔE^{FT98}
H_2	109.5	113.2	104.6	105.5	109.4	109.6	114.5	108.7	106.3	112.5
LiH	57.8	61.0	53.5	53.4	58.1	56.9	58.4	53.9	54.5	55.2
CH_4	419.3	462.3	419.8	410.6	416.6	417.7	421.1	411.5	421.4	419.9
NH_3	297.4	337.3	301.7	293.2	301.4	295.2	298.8	292.9	296.4	295.5
OH	106.4	124.1	109.8	106.3	109.6	106.8	107.8	106.0	107.6	105.0
H_2O	232.2	266.5	234.2	226.6	232.5	231.8	230.1	227.3	231.5	226.1
HF	140.8	162.2	142.0	137.5	141.0	143.6	138.7	138.0	141.9	137.8
Li_2	24.4	23.9	19.9	20.2	20.5	21.3	22.5	20.5	22.7	15.0
LiF	138.9	156.1	138.6	132.9	140.1	136.9	128.0	128.5	136.6	130.4
Be_2	3.0	12.8	9.8	7.9	6.1	5.6	4.5	5.8	9.4	6.3
C_2H_2	405.4	460.3	414.9	400.4	405.3	405.1	401.2	397.0	408.1	402.7
C_2H_4	562.6	632.6	571.5	554.5	560.7	561.5	561.5	552.0	565.3	563.5
HCN	311.9	361.0	326.1	313.6	320.3	312.8	311.8	309.6	312.4	312.5
CO	259.3	299.1	268.8	257.9	261.8	260.6	256.0	255.9	258.8	254.7
N_2	228.5	267.4	243.2	232.7	239.8	226.7	229.2	228.9	223.2	229.7
NO	152.9	198.7	171.9	161.6	166.0	158.3	158.5	158.5	152.2	158.7
O_2	120.5	175.0	143.7	133.3	135.3	135.7	131.4	132.0	128.1	132.2
F_2	38.5	78.2	53.4	45.6	49.4	46.7	43.2	43.9	39.7	46.5
P_2	117.3	143.8	121.1	114.1	121.0	111.2	117.8	117.5	114.6	122.4
Cl_2	58.0	83.0	65.1	58.9	57.2	57.9	59.4	59.6	54.6	60.1
mae	—	31.7	7.9	4.9	4.3	2.8	3.1	4.6	2.5	4.1
mare (in %)	—	21.7	7.4	4.5	4.5	3.4	3.0	4.0	2.2	5.5

[a]All functionals were evaluated on PBE-xc orbitals and densities at experimental geometries. Zero-point vibration has been removed from experimental energies [13]. See caption of Table III.

or HCN) and sometimes bad (as for CH_4 or H_2O). BLYP and HCTH also perform well for the singly bonded molecules and not quite so well for the multiply bonded ones. The mean absolute error for the 20 atomization energies is reduced to 8 kcal/mol for PBE, 5 kcal/mol for RPBE, 4 kcal/mol for BLYP, and 3 kcal/mol for HCTH. Atomization energies (including those of most of the molecules in our list) have been used to fit the 18 parameters in the HCTH functional, and so one has to expect a good performance for this quantity. Despite the large number of fit parameters, the HCTH atomization energies are only slightly better than those of functionals with far fewer fitting parameters.

The meta-GGAs in general perform well for atomization energies and typically do not exhibit any preferential overbinding for singly or multiply bonded molecules. The mean absolute errors range from less than 3 kcal/mol for VS98 to less than 5 kcal/mol for KCIS. The KCIS functional might have performed better if the parameter in its exchange part (i.e., the PKZB exchange) had been reoptimized to minimize the mean absolute error

for the atomization energies. Just as for the GGAs, the improvement that can be achieved by using a large number of fit parameters (as in VS98) is also limited: PKZB, which contains only one parameter fitted to chemical data, performs almost as well as VS98, which contains 21.

It is interesting to note that all the functionals tested in this work show larger errors for the atomization energy of O_2. Gunnarsson and Jones [84] have argued that the interaction of the occupied antibonding (and highly noded) $1\pi_g$ orbital with the lower energy shell is not described correctly in LSD. This argument probably also holds for the GGAs and meta-GGAs.

JELLIUM SURFACES

Metal surface energies are like and yet unlike molecular atomization energies. When a bond is broken in a molecule or solid, new surface area is created around the divorced atoms, at some cost in energy. But the Kohn–Sham orbital energies are continuous and the electron correlations are very long-ranged only at the metal surface. Local and

semilocal functionals can be expected to work better when the orbital energies are continuous, but worse when correlations are long-ranged.

The first self-consistent calculations for the jellium surface were reported by Lang and Kohn [85], who used the LSD approximation for exchange and correlation. However, since the exact solution for the jellium surface is not known, the magnitude of the surface exchange and correlation energy continues to be a matter of debate. The problem has been studied with various methods such as wave-vector analysis [86], the Fermi hypernetted chain approximation [87], and diffusion Monte Carlo [88]. Recently, Pitarke and Eguiluz [89] calculated the surface exchange and correlation energies within the random-phase approximation (RPA). With their study, exact surface exchange energies became available. Based on the results of Pitarke and Eguiluz, Kurth and Perdew [90] estimated the surface exchange-correlation energy, σ_{xc}, beyond RPA by including a GGA ''short-range'' correction to RPA. This estimate turns out to be close to the total surface exchange-correlation energy in LSD, although the individual LSD exchange and correlation pieces are seriously in error.

For the present study, we have calculated the surface exchange and correlation energies from the approximate exchange–correlation functionals of the second section. The results are shown in Tables V and VI, respectively. Surface exchange energies are overestimated by LSD, the error ranging from 16% at $r_s = 2$ to almost 100% at $r_s = 6$. This error is reduced by the PBE, RPBE, and BLYP GGAs, with PBE performing best among these approxi-

mations. RPBE and BLYP give essentially the same results for σ_x. The fourth GGA we tested, HCTH, gives surface exchange energies which are even more in error than LSD over most of the range of r_s values. Among the meta-GGAs, PKZB and FT98 underestimate σ_x while VS98 typically overestimates it. While FT98 is consistently worse than the PBE GGA, PKZB is consistently better. The fact that FT98 even gives a negative surface exchange energy for $r_s = 6$ is probably attributable to a wrong fourth-order gradient coefficient in the slowly varying limit. Overall, VS98 gives the best approximation of σ_x for low densities ($r_s \geq 4$), while PKZB yields the best results for higher densities ($r_s < 4$).

The results for the surface correlation energies (Table VI) vary strongly over the different approximations to the correlation functional. Although exact results are not available, we believe that the results of the first column, which were obtained by combining a refined GGA short-range correlation correction [91] with the RPA results of Pitarke and Eguiluz [89], give an accurate estimate for σ_c. The PBE GGA and the PKZB meta-GGA (which was constructed to leave the PBE surface correlation energies essentially unchanged) give the results closest to this estimate. KCIS surface correlation energies are somewhat higher than those from PBE, but still in a similar range. LSD surface correlation energies are too low, but VS98 and HCTH results are even lower. The latter functional (HCTH) even gives negative surface correlation energies. BLYP also shows little improvement over LSD results. Finally, FT98 seriously overestimates surface correlation energies.

TABLE V

Surface exchange energies (in erg / cm^2) for jellium using self-consistent LSD-xc orbitals and densities.[a]

r_s	σ_x^{exact}	σ_x^{LSD}	σ_x^{PBE}	σ_x^{RPBE}	σ_x^{BLYP}	σ_x^{HCTH}	σ_x^{PKZB}	σ_x^{VS98}	σ_x^{FT98}
2.00	2624	3037	2438	2380	2380	3338	2578	2859	2428
2.07	2296	2674	2127	2073	2073	2933	2252	2501	2114
2.30	1521	1809	1395	1353	1354	1970	1484	1657	1375
2.66	854	1051	770	740	742	1131	825	929	745
3.00	526	669	468	445	447	715	505	574	441
3.28	364	477	318	300	301	503	346	396	291
4.00	157	222	128	117	118	226	142	167	103
5.00	57	92	40	34	34	89	47	59	19
6.00	22	43	12	7	8	39	15	21	−7
mare (in %)		36.7	16.7	23.4	22.7	40.9	8.6	7.6	34.1

[a]Exact surface exchange energies were provided by Pitarke and Eguiluz [89, 112]. (1 hartree / bohr^2 = 1.557 × 10^6 erg / cm^2)

TABLE VI _____

Surface correlation energies (in erg / cm²) for jellium using self-consistent LSD-xc orbitals and densities.[a]

r_s	σ_c"exact"	σ_c^{LSD}	σ_c^{PBE}	σ_c^{BLYP}	σ_c^{HCTH}	σ_c^{PKZB}	σ_c^{KCIS}	σ_c^{VS98}	σ_c^{FT98}
2.00	789	317	827	388	−114	824	939	204	1127
2.07	719	287	754	350	−106	750	857	186	1034
2.30	539	210	567	254	−84	564	649	138	795
2.66	360	137	382	161	−61	380	441	90	554
3.00	255	95	275	109	−47	274	320	62	410
3.28	199	72	215	80	−38	214	252	47	329
4.00	111	39	124	40	−24	124	148	24	200
5.00	56	19	67	17	−14	66	81	10	115
6.00	33	10	40	8	−10	40	49	4	73
mare (in %)		63.3	9.9	59.6	119.6	9.4	28.9	77.6	69.0

[a]"Exact" results are from [91].

Table VII shows the combined surface exchange–correlation energy σ_{xc}. Because of the long-range nature of exchange and correlation at the surface, the errors of semilocal functionals for exchange and for correlation are expected to show considerable cancellation in σ_{xc}. With the exception of BLYP, all functionals that we tested in this study show this error cancellation, which is especially remarkable for LSD: LSD surface exchange–correlation energies are within 2% of the estimated exact values, while σ_x^{LSD} is in error by 15–100% and σ_c^{LSD} by 60–330%. Of all the functionals tested, only PKZB performs better than LSD here. All other functionals perform worse for σ_{xc}, with BLYP giving results particularly off the mark. Note also that the RPBE, which improves upon PBE for molecular atomization energies, worsens the surface energies. Because σ_{xc} is about three times bigger than the total surface energy σ for typical metals, it must, of course, be calculated accurately.

The PKZB meta-GGA surface exchange–correlation energies for jellium preceded but are supported by *two* independent estimates of the exact σ_{xc}: (1) a short-range correction to exact exchange and RPA correlation [91] and (2) a long-range correction to GGA exchange–correlation [91]. While we have chosen (1) as our "exact" standard here, an alternative "exact" standard would be the diffusion Monte Carlo values of Ref. [88], which are 5% higher at $r_s = 2$ and 46% higher at $r_s = 4$. Of the nine density functionals tested here, only KCIS and FT98 are closer than PKZB to this alternative "exact" standard, and none is close at $r_s = 4$.

Functionals that predict the right σ_{xc} need to be right or nearly right in the slowly varying limit.

The extraordinary accuracy of the PKZB functional for σ_{xc} seems to reflect its use of the correct gradient coefficients for exchange and correlation. Using the right second-order gradient coefficient for the exchange energy introduces some error into the exchange energies of atoms (Table I) but does no harm to the atomization energies of molecules (Table IV), and leads to highly accurate surface energies (Table VII).

SOLIDS

Bulk solids, especially simple metals, have rather slowly varying valence electron densities for which the LSD and GGA descriptions are almost equivalent, at least for those exchange-correlation functionals that properly recover the uniform-gas limit [74, 92, 93]. As a result, LSD is still very popular in solid-state physics. (For the valence–valence exchange energy, without correlation, GGA is considerably better than LSD [93, 94].)

Nevertheless, the accurate calculation of lattice constants and bulk moduli remains a challenge to all semilocal functionals [95–97], for reasons we shall discuss. The lattice constants or equilibrium unit cell volumes V_0 are found by minimizing the total energy E per cell as a function of the cell volume:

$$\left. \frac{\partial E}{\partial V} \right|_{V_0} = 0. \qquad (22)$$

More generally,

$$P = - \left. \frac{\partial E}{\partial V} \right|_V \qquad (23)$$

TABLE VII

Surface exchange–correlation energies (in erg / cm^2) for jellium using self-consistent LSD-xc orbitals and densities.[a]

r_s	σ_{xc}"exact"	σ_{xc}^{LSD}	σ_{xc}^{PBE}	σ_{xc}^{RPBE}	σ_{xc}^{BLYP}	σ_{xc}^{HCTH}	σ_{xc}^{PKZB}	σ_{xc}^{KCIS}	σ_{xc}^{VS98}	σ_{xc}^{FT98}
2.00	3413	3354	3265	3207	2768	3224	3402	3517	3063	3555
2.07	3015	2961	2881	2827	2423	2827	3002	3109	2687	3148
2.30	2060	2019	1962	1920	1608	1886	2048	2133	1795	2170
2.66	1214	1188	1152	1122	903	1070	1205	1266	1019	1299
3.00	781	764	743	720	556	668	779	825	636	851
3.28	563	549	533	515	381	465	560	598	443	620
4.00	268	261	252	241	158	202	266	290	191	303
5.00	113	111	107	101	51	75	113	128	69	134
6.00	54	53	52	47	16	29	55	64	25	66
mare (in %)		2.1	4.9	8.5	34.8	18.7	0.6	7.3	23.5	10.4

[a]"Exact" results are from [91].

is the pressure at volume V. The bulk modulus of elastic stiffness is

$$B_0 = -V \frac{\partial P}{\partial V}\bigg|_{V_0}. \quad (24)$$

We have calculated the zero-temperature V_0 and B_0 in a standard way, by fitting the calculated $E(V)$ (typically 6–8 points in the range $0.90 \lesssim V/V_0 \lesssim 1.05$) to the analytic Murnaghan equation of state [98] and then differentiating this equation.

By Eq. (22), $E(V)$ is flat near V_0, so any small volume-dependent error in the approximate en-

ergy can shift the equilibrium volume away from experiment. For LSD, GGA, and related functionals, this error seems to come not from the valence–valence but from the core–valence interaction [92]. This interaction occurs in a narrow intershell region in which the density switches rapidly from one exponential decay to another.

Our calculated equilibrium volumes V_0 and bulk moduli B_0 are presented in Tables VIII and IX, respectively. The LSD and PBE-GGA calculations are self-consistent within the scalar-relativistic linearized augmented plane-wave (LAPW) method [99]. The other GGAs and meta-GGAs

TABLE VIII

Equilibrium unit cell volumes V_0 (in bohr^3) for bulk solids, using self-consistent LSD-xc orbitals and densities for LSD, and self-consistent PBE-GGA-xc orbitals and densities for the other functionals.[a]

Solid	V_0^{expt}	V_0^{LSD}	V_0^{PBE}	V_0^{RPBE}	V_0^{BLYP}	V_0^{HCTH}	V_0^{PKZB}	V_0^{KCIS}	V_0^{VS98}	V_0^{FT98}
Na	255.4	224.4	249.8	267.8	250.1	275.6	272.0	271.0	229.1	194.0
NaCl	302.7	276.1	313.1	338.3	324.3	353.6	296.6	312.5	240.0	321.0
Al	112.1	106.6	111.2	113.3	116.5	108.4	109.3	108.0	101.8	106.0
Si	270.0	266.2	276.3	282.1	285.6	278.3	274.5	280.4	270.6	268.1
Ge	305.9	301.4	322.1	331.0	343.1	328.9	314.6	319.9	318.1	325.4
GaAs	304.3	298.3	320.5	330.2	340.1	329.0	314.0	319.4	315.8	323.0
Cu	78.7	73.5	80.6	83.5	85.7	82.5	78.5	79.9	82.7	78.7
W	106.5	104.0	108.9	110.2	112.7	106.1	107.1	108.1	108.9	106.9
Fe	79.5	70.5	76.7	79.1	80.3	—	75.9	77.0	—	75.5
Pd	99.3	95.5	103.2	106.1	110.1	104.3	100.9	102.9	110.0	106.9
Pt	101.3	99.7	105.7	107.5	112.4	104.4	103.0	104.4	110.2	106.8
Au	112.8	111.9	121.1	124.6	131.0	123.5	117.8	120.6	129.2	120.8
mare (in %)	—	4.8	3.6	6.0	8.0	6.3	2.6	3.8	8.1	6.2

[a]The calculations were done with the WIEN code [99]. The experimental values are from Refs. [92] (for most of the solids), [113] (for Pd), and [95] (for Pt and Au). For Fe, the HCTH and VS98 energies oscillate near the minimum.

TABLE IX _____

Equilibrium bulk moduli B_0 (in GPa) for bulk solids.[a]

Solid	B_0^{expt}	B_0^{LSD}	B_0^{PBE}	B_0^{RPBE}	B_0^{BLYP}	B_0^{HCTH}	B_0^{PKZB}	B_0^{KCIS}	B_0^{VS98}	B_0^{FT98}
Na	6.9	9.2	7.6	6.6	7.1	6.1	7.0	7.0	12.5	15.1
NaCl	24.5	32.2	23.4	19.9	22.1	17.0	28.1	27.1	98.0	23.0
Al	77.3	84.0	77.3	75.6	58.6	86.8	90.5	97.8	106.0	61.6
Si	98.8	97.0	89.0	85.5	79.2	86.0	93.6	89.7	104.	97.8
Ge	76.8	71.2	59.9	56.1	48.0	54.1	64.6	61.2	64.3	58.1
GaAs	74.8	74.3	60.7	55.5	49.8	53.5	65.1	61.1	68.3	57.0
Cu	138	191	139	124	113	114	154	144	118	198
W	310	335	298	293	272	312	311	313	299	317
Fe	172	259	198	164	161	—	198	184	—	213
Pd	181	226	174	154	140	142	181	165	130	317
Pt	283	312	247	229	200	227	267	253	210	272
Au	172	195	142	122	101	111	153	137	108	155
mare (in %)	—	19.1	9.9	14.6	21.5	20.0	9.3	11.5	50.7	29.4

[a] See footnote for Table VIII.

have been evaluated on the PBE-GGA densities and orbitals. Note that B_0 was evaluated at the theoretical volume V_0, which can be the main source of error in the theoretical bulk modulus. Generally, the more V_0 is overestimated in comparison to experiment, the more B_0 is underestimated.

While LSD tends to underestimate the equilibrium volume V_0, GGA tends to overestimate it, with the least overestimation provided by PBE and the most by BLYP. Among the meta-GGAs, PKZB and KCIS are the best performers, although they clearly leave room for improvement. Recovery of the correct uniform-gas limit seems to be a necessary condition for the accurate calculation of V_0 and B_0 [100]. Because the errors in V_0 are believed to come from the core–valence interaction [92], they can in principle be removed by constructing an electron–ion pseudopotential beyond the level of semilocal approximations [101–103].

Somewhat contrarily to popular belief, the PBE-GGA and PKZB meta-GGA results for V_0 and B_0 improve upon those of LSD, and turn out to be the second-best and best functionals tested for this purpose. However, the improvements are statistical and not uniform. Some of the semiempirical functionals fail badly for solids.

Discussion and Conclusions

In this work, we have presented results from extensive numerical tests of nine approximate exchange–correlation functionals. These approximations (other than LSD) were all of the GGA or meta-GGA form, but their constructions followed very different philosophies. Some of the functionals were constructed to preserve key properties of the exact exchange–correlation functional. Others followed a more empirical path and used a (sometimes large) number of parameters obtained by fitting the numerical results to experimental data, typically for either atomic or molecular systems.

Not surprisingly, with the latter approach one can obtain a functional which performs well for atomic and molecular systems. However, the improvement that can be achieved in this way appears to be limited and does not scale linearly with the number of fit parameters. For example, the HCTH and VS98 functionals are both highly parametrized with 18 and 21 fit parameters, respectively. Although HCTH and VS98 give the smallest mean absolute errors for the atomization energies of our set of molecules, the PKZB functional, which was constructed by preserving many exact properties and contains only one parameter fitted to chemical data, performs almost as well for molecular atomization energies. (Tests of PKZB for the extended G2 data set have recently been performed [104].)

It is a challenge for all functionals to perform well both for small systems such as atoms and molecules and for extended systems such as surfaces and solids. In our study, we find that this challenge is best met by those functionals designed to incorporate key exact properties (such as PBE

among the GGAs and PKZB among the meta-GGAs). Even the popular BLYP GGA, which gives very good results for atoms and molecules, performs rather poorly for surface correlation energies. Surface correlation energies are apparently hard to get right. All the functionals obtained by fitting to atomic and molecular data (BLYP, HCTH, VS98, and FT98) are seriously in error for surfaces and for bulk solids, often much more so than LSD.

We favor a conservative philosophy to approximate the universal exchange–correlation functional: Retain all exact conditions that are already satisfied, and add additional ones which have been neglected in previous approximations. This approach should lead to improved (or at least not worsened) performance for a wide variety of systems, and at the same time provide some physical insight into the reasons for this improvement. For example, the improved performance of PKZB over PBE could be attributed to the incorporation of two additional exact properties: (1) no self-correlation error for one-electron systems and (2) correct fourth-order gradient expansion for the exchange functional.

On the other hand, adding more empirical parameters to an approximate functional without providing new physical arguments to support its form may lead to a somewhat higher accuracy for a particular class of systems but will most likely not help to improve functional performance for physically different systems.

As is well known, GGAs greatly improve upon the LSD description of atoms and molecules, although their second-order gradient coefficient for exchange is usually about twice as big as the first-principles gradient coefficient [34]. It is not so well-known that these GGAs typically worsen the LSD description of the metal surface energy. However, a meta-GGA (PKZB) with the correct gradient expansion is able to bring good improvement over LSD in both cases, probably because of its ability to discriminate between iso-orbital and orbital overlap regions. Apart from one unknown fourth-order gradient coefficient fitted to molecular atomization energies, this meta-GGA is an entirely theoretical construct. Further tests and theoretical extensions are under consideration. It remains to be seen if the PKZB meta-GGA can match the good PBE GGA performance for the description of pressure-driven phase transitions in solids [105], hydrogen bonds [106], and van der Waals bonds [107, 108].

In the tests we have made here, the PKZB meta-GGA has rather consistently improved upon the PBE GGA. We believe that this is a consequence of the more general meta-GGA form [Eq. (8) instead of Eq. (7)]. Attempts to revise the PBE that stay within the GGA form [Eq. (7)] tend to improve some properties while worsening others. For example, improved GGA atomization energies of molecules [63, 64] lead to worsened surface energies and lattice constants, while improved lattice constants [109] worsen the atomization energies.

We recommend that the results of density functional calculations be reported at all three levels: LSD, PBE GGA, and PKZB meta-GGA.

Appendix A: KCIS Correlation Energy Functional

In this appendix, we give formulas for the KCIS correlation energy functional [25]. It can be written in the following self-interaction-free way:

$$
E_c^{\text{KCIS}} = \int d^3r \Bigg\{ n(\mathbf{r}) \epsilon_c^{\text{GGAGAP}}(n_\uparrow, n_\downarrow, \nabla n)
$$
$$
- \sum_\sigma \frac{\tau_\sigma^W(\mathbf{r})}{\tau_\sigma(\mathbf{r})} n_\sigma(\mathbf{r}) \epsilon_c^{\text{GGAGAP}}(n_\sigma, 0, \nabla n_\sigma) \Bigg\}, \quad \text{(A1)}
$$

where τ_σ^W is given in Eq. (19). The function $\epsilon_c^{\text{GGAGAP}}$ has the spin-polarization dependence

$$
\epsilon_c^{\text{GGAGAP}}(n_\uparrow, n_\downarrow, g)
$$
$$
= \epsilon_c^{\text{GAP,unp}}(r_s, g, G)
$$
$$
+ f(\zeta)\big[\epsilon_c^{\text{GAP,pol}}(r_s, g, G)
$$
$$
- \epsilon_c^{\text{GAP,unp}}(r_s, g, G)\big], \quad \text{(A2)}
$$

with

$$
f(\zeta) = \frac{(1+\zeta)^{4/3} + (1-\zeta)^{4/3} - 2}{2(2^{1/3}-1)}. \quad \text{(A3)}
$$

The gap G in Eq. (A2) is related to $g = |\nabla n|$ by

$$
G = \frac{g^2}{8n^2}. \quad \text{(A4)}
$$

The functions $\epsilon_c^{\text{GAP,unp}}$ and $\epsilon_c^{\text{GAP,pol}}$ are only defined for the unpolarized or fully spin-polarized

situation, respectively. They read

$$\epsilon_c^{\mathrm{GAP,\,unp}}(r_s, g, G) = \frac{\epsilon_c^{\mathrm{GGA,\,unp}}(r_s, g) + c_1(r_s)G}{1 + c_2(r_s)G + c_3(r_s)G^2}$$
(A5)

and

$$\epsilon_c^{\mathrm{GAP,\,pol}}(r_s, g, G)$$
$$= \frac{\epsilon_c^{\mathrm{GGA,\,pol}}(r_s, g) + 0.7c_1(r_s)G}{1 + 1.5c_2(r_s)G + 2.59c_3(r_s)G^2}.$$
(A6)

The $c_i(r_s)$ are parametrized functions [110] obtained from a model of a uniform electron gas with a gap G in the excitation spectrum. In Eqs. (A5) and (A6), the functions $\epsilon_c^{\mathrm{GGA,\,unp}}(r_s, g)$ and $\epsilon_c^{\mathrm{GGA,\,pol}}(r_s, g)$ are given by

$$\epsilon_c^{\mathrm{GGA,\,unp}}(r_s, g)$$
$$= \frac{\epsilon_c^{\mathrm{unif}}(r_s, \zeta = 0)}{1 + \beta \ln(1 + t^2/|\epsilon_c^{\mathrm{unif}}(r_s, \zeta = 0)|)}$$
(A7)

and

$$\epsilon_c^{\mathrm{GGA,\,pol}}(r_s, g)$$
$$= \frac{\epsilon_c^{\mathrm{unif}}(r_s, \zeta = 1)}{1 + \beta \ln(1 + 2^{-1/3}t^2/|\epsilon_c^{\mathrm{unif}}(r_s, \zeta = 1)|)},$$
(A8)

respectively. Here, $\epsilon_c^{\mathrm{unif}}$ is the usual correlation energy per particle of a uniform electron gas without gap, and $\beta = 0.066725$ is the second-order gradient coefficient for correlation in the high-density limit. Finally

$$t = \frac{\pi^{4/3}}{3}\left(\frac{2}{3}\right)^{1/3} r_s^{7/2} g = \frac{g}{2k_s n}$$
(A9)

is another reduced density gradient, where $k_s = (4k_F/\pi)^{1/2}$ and $k_F = (3\pi^2 n)^{1/3}$.

KCIS have developed Eqs. (A5) and (A6) for $r_s \lesssim 10$. We have found a peculiarity of their expressions for $r_s \gg 10$, which is also evident in Figure 4:

$$\lim_{s \to 0} \lim_{r_s \to \infty} \epsilon_c^{\mathrm{GAP,\,pol}}(r_s, g, g^2/8n)$$
$$\neq \lim_{r_s \to \infty} \lim_{s \to 0} \epsilon_c^{\mathrm{GAP,\,pol}}(r_s, g, g^2/8n),$$
(A10)

with s defined by Eq. (13).

Appendix B: Lower Bound on the Kinetic Energy Density

Here we briefly prove the lower bound of Eq. (21) on the kinetic energy density. We start with the Weizsäcker kinetic energy density

$$\tau_\sigma^W = \frac{|\nabla n_\sigma|^2}{8n_\sigma}$$
$$= \frac{1}{8n_\sigma}\left|\sum_i^{\mathrm{occ}} 2\varphi_{i\sigma}\nabla\varphi_{i\sigma}\right|^2 \leq \frac{1}{2n_\sigma}\left(\sum_i^{\mathrm{occ}} |\varphi_{i\sigma}||\nabla\varphi_{i\sigma}|\right)^2$$
(B1)

where we assume real single-particle orbitals. Using the Cauchy–Schwarz inequality,

$$\left|\sum_i \alpha_i^* \beta_i\right|^2 \leq \left(\sum_i |\alpha_i|^2\right)\left(\sum_i |\beta_i|^2\right),$$
(B2)

we obtain from Eq. (B1)

$$\tau_\sigma^W \leq \frac{1}{2n_\sigma}\left(\sum_i^{\mathrm{occ}} |\varphi_{i\sigma}|^2\right)\left(\sum_j^{\mathrm{occ}} |\nabla\varphi_{j\sigma}|^2\right) = \tau_\sigma,$$
(B3)

which completes the proof of Eq. (21).

References

1. Hohenberg, P.; Kohn, W. Phys Rev B 1964, 136, 864.
2. Kohn, W.; Sham, L. J. Phys Rev A 1965, 140, 1133.
3. Dreizler, R. M.; Gross, E. K. U. Density Functional Theory; Springer: Berlin, 1990.
4. Parr, R. G.; Yang, W. Density-Functional Theory of Atoms and Molecules; Oxford University Press: New York, 1989.
5. von Barth, U.; Hedin, L. J Phys C 1972, 5, 1629.
6. Ceperley, D. M.; Alder, B. J. Phys Rev Lett 1980, 45, 566.
7. Langreth, D. C.; Mehl, M. J. Phys Rev B 1983, 28, 1809.

8. Perdew, J. P. Phys Rev B 1986, 33, 8822; Ibid. E 1986, 34, 7406.

9. Perdew, J. P.; Wang, Y. Phys Rev B 1986, 33, 8800; Ibid. E 1989, 40, 3399.

10. Becke, A. D. Phys Rev A 1988, 38, 3098.

11. Lee, C.; Yang, W.; Parr, R. G. Phys Rev B 1988, 37, 785.

12. Perdew, J. P. in Electronic Structure of Solids '91, Ziesche, P.; Eschrig, H. Eds.; Akademie: Berlin, 1991, p. 11.

13. Perdew, J. P.; Burke, K.; Ernzerhof, M. Phys Rev Lett 1996, 77, 3865; Ibid. E 1997, 78, 1396.

14. Becke, A. D. J Chem Phys 1988, 88, 1053.

15. Tschinke, V.; Ziegler, T. Can J Chem 1989, 67, 460.

16. Becke, A. D.; Roussel, M. R. Phys Rev A 1989, 39, 3761.

17. Dobson, J. F. J Phys Condens Matt 1992, 4, 7877.

18. Engel, E.; Vosko, S. H. Phys Rev B 1994, 50, 10498.

19. Umrigar, C. J.; Gonze, X. Phys Rev A 1994, 50, 3827.

20. Proynov, E. I.; Ruiz, E.; Vela, A.; Salahub, D. R. Int J Quant Chem Symp 1995, 29, 61.

21. Neumann, R.; Handy, N. C. Chem Phys Lett 1997, 266, 16.

22. Proynov, E. I.; Sirois, S.; Salahub, D. R. Int J Quant Chem 1998, 64, 427.

23. Van Voorhis, T.; Scuseria, G. E. J Chem Phys 1998, 109, 400.

24. Filatov, M.; Thiel, W. Phys Rev A 1998, 57, 189. Note that the first line of Eq. (28) in Ref. [24] is mistyped.

25. Krieger, J. B.; Chen, J.; Iafrate, G. J.; Savin, A. In Electron Correlations and Materials Properties; Gonis, A.; Kioussis, N., Eds.; Plenum: New York, 1999.

26. Perdew, J. P.; Kurth, S.; Zupan, A.; Blaha, P. Phys Rev Lett 1999, 82, 2544; Ibid E 1999, 82, 5179.

27. Ernzerhof, M.; Scuseria, G. E. J Chem Phys 1999, 111, 911.

28. Colle, R.; Salvetti, O. J Chem Phys 1983, 79, 1404.

29. Morrison, R. C. Int J Quant Chem 1993, 46, 583.

30. Singh, R.; Massa, L.; Sahni, V. preprint.

31. Skyrme, T. H. R. Nucl Phys 1959, 9, 615.

32. Perdew, J. P. Phys Rev Lett 1985, 55, 1665.

33. Ghosh, S. K.; Parr, R. G. Phys Rev A 1986, 34, 785.

34. Svendsen, P. S.; von Barth, U. Phys Rev B 1996, 54, 17402.

35. Becke, A. D. J Chem Phys 1993, 98, 1372.

36. Becke, A. D. J Chem Phys 1993, 98, 5648.

37. Becke, A. D. J Chem Phys 1998, 109, 8188.

38. Perdew, J. P.; Ernzerhof, M.; Burke, K. J Chem Phys 1996, 105, 9982.

39. Ernzerhof, M. Chem Phys Lett 1996, 263, 499.

40. Burke, K.; Ernzerhof, M.; Perdew, J. P. Chem Phys Lett. 1997, 265, 115.

41. Ernzerhof, M.; Scuseria, G. E. J Chem Phys 1999, 110, 5029.

42. Adamo, C.; Barone, V. J Chem Phys 1999, 110, 6158.

43. Kohn, W. private communication.

44. Perdew, J. P.; Chevary, J. A.; Vosko, S. H.; Jackson, K. A.; Pederson, M. R.; Singh, D. J.; Fiolhais, C. Phys Rev B 1992, 46, 6671; Ibid E 1993, 48, 4978.

45. Becke, A. D. J Chem Phys 1997, 107, 8554.

46. Fan, L.; Ziegler, T. J Chem Phys 1991, 94, 6057.

47. Talman, J. D.; Shadwick, W. F. Phys Rev A 1976, 14, 36.

48. Engel, E.; Dreizler, R. M. J Comp Chem 1999, 20, 31.

49. Grabo, T.; Kreibich, T.; Kurth, S.; Gross, E. K. U. In The Strong Coulomb Correlations and Electronic Structure Calculations: Beyond Local Density Approximations; Anisimov, V., Ed.; Gordon and Breach: Amsterdam, to appear.

50. Neumann, R.; Nobes, R. H.; Handy, N. C. Mol Phys 1996, 87, 1.

51. Vosko, S. H.; Wilk, L.; Nusair, M. Can J Phys 1980, 58, 1200.

52. Perdew, J. P.; Zunger, A. Phys Rev B 1981, 23, 5048.

53. Perdew, J. P.; Wang, Y. Phys Rev B 1992, 45, 13244.

54. Burke, K.; Perdew, J. P.; Ernzerhof, M. J Chem Phys 1998; 109, 3760.

55. Lieb, E. H.; Oxford, S. Int J Quant Chem 1981, 19, 427.

56. Moroni, S.; Ceperley, D. M.; Senatore, G. Phys Rev Lett 1995, 75, 689.

57. Levy, M.; Perdew, J. P. Phys Rev B 1993, 48, 11638; Ibid. E 1997, 55, 13321.

58. Ma, S.-K., Brueckner, K. A. Phys Rev B 1977, 13, 1477.

59. Rasolt, M.; Geldart, D. J. W. Phys Rev B 1986, 34, 1325.

60. Langreth, D. C.; Perdew, J. P. Phys Rev B 1980, 21, 5469.

61. Levy, M. Int J Quant Chem Symp 1989, 23, 617.

62. Perdew, J. P.; Burke, K.; Wang, Y. Phys Rev B 1996, 54, 16533; Ibid. E 1998, 57, 14999.

63. Hammer, B.; Hansen, L. B.; Norskov, J. K. Phys Rev B 1999, 59, 7413.

64. Zhang, Y.; Yang, W. Phys Rev Lett 1998, 80, 890.

65. Perdew, J. P.; Burke, K.; Ernzerhof, M. Phys Rev Lett 1998, 80, 891.

66. Zupan, A.; Burke, K.; Ernzerhof, M.; Perdew, J. P. J Chem Phys 1997, 106, 10184.

67. Colle, R.; Salvetti, O. Theoret Chim Acta 1975, 37, 329.

68. Hamprecht, F. A.; Cohen, A. J.; Tozer, D. J.; Handy, N. C. J Chem Phys 1998, 109, 6264.

69. Perdew, J. P.; Burke, K. Int J Quant Chem 1996, 57, 309.

70. Brack, M.; Jennings, B. K.; Chu, Y. H. Phys Lett 1976, 65 B, 1.

71. Becke, A. D. J Chem Phys 1998, 109, 2092.

72. Becke, A. D. Int J Quant Chem 1983, 23, 1915.

73. Jones, R. O.; Gunnarsson, O. Phys Rev Lett 1985, 55, 107.

74. Perdew, J. P.; Ernzerhof, M.; Zupan, A.; Burke, K. J Chem Phys 1998, 108, 1522.

75. Seidl, M.; Perdew, J. P.; Levy, M. Phys Rev A 1999, 59, 51.

76. Yan, Z.; Perdew, J. P. work in progress.

77. Negele, J. W.; Vautherin, D. Phys Rev C 1972, 5, 1472.

78. Negele, J. W.; Vautherin, D. Phys Rev C 1975, 11, 1031.

79. Filatov, M.; Thiel, W. Int J Quant Chem 1997, 62, 603. Note that Eq. (19) of (79) is mistyped. The correct equation is Eq. (21) of M. Filatov and W. Thiel Mol Phys 1997, 91, 847.

80. Becke, A. D.; Edgecombe, K. E. J Chem Phys 1990, 92, 5397.

81. Kohn, W.; Mattsson, A. E. Phys Rev Lett 1998, 81, 3487.

82. Ortiz, G.; Souza, I.; Martin, R. M.; Phys Rev Lett 1998, 80, 353.

83. Ernzerhof, M.; Perdew, J. P.; Burke, K. Int J Quant Chem 1997, 64, 285.

84. Gunnarsson, O.; Jones, R. O. Phys Rev B 1985, 31, 7588.

85. Lang, N. D.; Kohn, W. Phys Rev B 1970, 1, 4555.

86. Langreth, D. C.; Perdew, J. P. Phys Rev B 1977, 15, 2884.

87. Krotscheck, E.; Kohn, W. Phys Rev Lett 1986, 57, 862.

88. Acioli, P. H.; Ceperley, D. M. Phys Rev B 1996, 54, 17199.

89. Pitarke, J. M.; Eguiluz, A. G. Phys Rev B 1998, 57, 6329.

90. Kurth, S.; Perdew, J. P. Phys Rev B 1999, 59, 10461.

91. Yan, Z.; Perdew, J. P.; Kurth, S. work in progress.

92. Fuchs, M.; Bockstedte, M.; Pehlke, E.; Scheffler, M. Phys Rev B 1998, 57, 2134.

93. Hood, R. Q.; Chou, M. Y.; Williamson, A. J.; Rajagopal, G.; Needs, R. J. Phys Rev B 1998, 57, 8972.

94. Städele, M.; Majewski, J. A.; Vogl, P.; Görling, A. Phys Rev Lett 1997, 79, 2089, Erratum unpublished.

95. Khein, A.; Singh, D. J.; Umrigar, C. Phys Rev B 1995, 51, 4105.

96. Trickey, S. B. Int J Quant Chem 1997, 61, 641.

97. Schmid, R. N.; Engel, E.; Dreizler, R. M.; Blaha, P.; Schwarz, K. Adv Quant Chem 1999, 33, 209.

98. Murnaghan, F. D. Proc Natl Acad Sci USA 1944, 30, 244.

99. Blaha, P.; Schwarz, K.; Luitz, J. WIEN 97, Technical University Vienna, 1997. [Improved and updated Unix version of the original copyrighted WIEN-code, which was published by P. Blaha, K. Schwarz, P. Sorantin, and S. B. Trickey, Comput. Phys. Commun. 59, 399 (1990)].

100. Kohler, B.; Fuchs, M.; Freihube, K.; Scheffler, M. Phys Rev A 1994, 49, 5152.

101. Bylander, D. M.; Kleinman, L. Phys Rev B 1997, 55, 9432.

102. Perdew, J. P. In Condensed Matter Theories 13; da Providencia, J.; Brajczewska, M., Eds.; Nova: New York, 1999.

103. Höck, A.; Engel, E. Phys Rev A 1998, 58, 3578.

104. Ernzerhof, M.; Adamo, C. private communication.

105. Zupan, A.; Blaha, P.; Schwarz, K.; Perdew, J. P. Phys Rev B 1998, 58, 11266.

106. Hamann, D. R. Phys Rev B 1997, 55, R10157.

107. Zhang, Y.; Pan, W.; Yang, W. J Chem Phys 1997, 107, 7921.

108. Patton, D. C.; Pederson, M. R. Phys Rev A 1997, 56, R2495.

109. Tinte, S.; Stachiotti, M. G.; Rodriguez, C. O.; Novikov, D. L.; Christensen, N. E. Phys Rev B 1998, 58, 11959.

110. Rey, J.; Savin, A. Int J Quant Chem 1998, 69, 581. After Eq. (32), the parameter a_2 is mistyped; it should be $a_2 = 1.07924$.

111. Amos, R. D.; Alberts, I. L.; Andrews, J. S.; Colwell, S. M.; Handy, N. C.; Jayatilaka, D.; Knowles, P. J.; Kobayashi, R.; Laming, G. J.; Lee, A. M.; Maslen, P. E.; Murray, C. W.; Palmieri, P.; Rice, J. E.; Sanz, J.; Simandiras, E. D.; Stone, A. J.; Su, M.-D.; Tozer, D. J. CADPAC6: The Cambridge Analytical Derivatives Package Issue 6.0 Cambridge, 1995.

112. Pitarke, J. M.; Eguiluz, A. G. unpublished.

113. Singh, D. J.; Askhenazi, J. Phys Rev B 1992, 46, 11570.